FY 2008 Report: June 2007 – May 2008

Radar Operations Center – Office of Hydrologic Development
Memorandum of Understanding

Dual-polarization solutions to QPE in partial radar beam blockage

David Riley, David Kitzmiller, and Dennis Miller

August 2008

Executive Summary

With the operational deployment of its RPG Build 11, scheduled to begin in late 2009, WSR-88D units will have the capability to estimate precipitation from dual polarization fields as well as via the traditional relationship based on horizontally-polarized reflectivity. An investigation has here been undertaken to determine if radar rainfall estimates based on the dual-polarization field Specific Differential Phase (Kdp) can be used to better infer rainfall in areas of partial beam blockage. Many WSR-88D coverage umbrellas presently feature such blockage zones, where horizontally-polarized reflectivity (Zh) is degraded and hence, rainfall intensity based on that field (i.e. R(Zh)) is consistently underestimated. These zones have lead to numerous artifacts in some operationally-generated, gridded precipitation products. Specific differential phase is determined solely from Doppler velocity information, which is less degraded by partial beam blockage than is reflectivity-based information. Based on earlier research findings, it is hoped that this quantity can be used to detect and estimate rainfall intensity (i.e. R(Kdp)) in zones where estimates based fully or partially on horizontal reflectivity may be seriously compromised.

Note that, while R(Kdp) is to be utilized under relatively limited conditions (i.e. where reflectivity echoes are deemed to be caused primarily by large raindrops or hail) in the WSR-88D rainfall estimation algorithm slated to be implemented operationally in RPG Build 11, the present investigation intends to look at the potential utility of R(Kdp) in more general circumstances. For example, in regions significantly affected by partial beam blockage, might R(Kdp) yield a more horizontally consistent and coherent field than estimates derived from reflectivity or differential reflectivity (i.e. R(Zh) or R(Zh, Zdr))?. Indeed, might R(Kdp) yield more worthwhile information even under precipitation conditions where it would not generally be the first choice for utilization in the operational precip estimation algorithm (such as in general stratiform rainfall conditions)?

Because WSR-88D prototypes have been based to date almost entirely in the flat-terrain area of Oklahoma, we obtained data collected by a radar of similar characteristics – i.e. NCAR's experimental, dual-polar, S-band unit known as S-Pol, during two of its deployments – i.e. in Colorado during the summer of 2006 and in Oregon during the winter of 2001. Both deployments were at locations where substantial portions of the radar umbrella experienced partial or total beam blockage. However, useful amounts of data were collected by volumetric scanning operations that enabled the partially blocked areas to be sampled by going to higher elevations.

Since the start of this study, methods for calculating specific differential phase were still being refined by staff of the National Severe Storms Laboratory. Furthermore, the input moment for the calculation, differential phase, is known to be statistically noisy. We have spent considerable time in evaluating results and refining sampling methodologies to get physically reasonable fields of specific differential phase. Ground-truth, rain

gauge-based rainfall estimates needed for the partially-blocked sectors are being collected from various sources.

We believe that our test datasets and analyses will yield valuable information on the utility of rainrate estimates based on specific differential phase.

Task 1: Dual-polarization solutions to QPE in partial radar beam blockage

This report covers progress on MOU Task 1 during the period June 2007-May 2008

Overview and Problem description

The aim of the study is to assess the utility of specific differential phase as a reliable indicator of rainrate under conditions of partial beam blockage. Motivation for the study is outlined in the attached Statement of Need.

Rainfall estimates from the Precipitation Processing System (PPS) of the WSR-88D radar have been used for years in operational, hydrological applications such as the Multisensor Precipitation Estimator (MPE) and the National Weather Service River Forecasting System (NWSRFS) to determine estimates of quantitative precipitation. At present, the effects of beam blockage (both partial and total) are based on application of a radar beam propagation model along with a digital elevation model (DEM). The model estimates the percentage of each azimuth beam at each elevation that is blocked by terrain, beginning with the lowest elevation, i.e. 0.5°. For those azimuths with more than partial blockage (the threshold usually being 50%), the QPE system obtains reflectivity from the next-higher elevation (typically 1.0-1.5°, depending on the volume coverage pattern). This logic continues searching upward until an unblocked (i.e. less than the threshold) elevation is encountered at that azimuth and range. This approach has the limitation that substantial reflectivity at low levels may go unutilized, and reflectivity profile effects generally introduce underestimation biases where higher elevation angles must be used. Alternative approaches, applicable when low-elevation beam blockage is partial but less than the threshold, rely on statistical corrections (i.e. power enhancements) to the beam reflectivity itself. These approaches cannot fully account for variations in the beam path caused by varying temperature and humidity profiles.

The specific differential phase (Kdp) radar moment is based solely on Doppler velocity information. The propagation speeds of the vertically and horizontally polarized beam pulses differ from each other within a mass of hydrometeors that are not perfectly spherical. Particularly for larger raindrops, the horizontally-polarized beam travels more slowly, since the drops are oblate and present a larger horizontal backscattering cross section when compared to the vertical polarization. The difference in propagation speeds appears as a phase shift (differential phase Φ) between the reflected horizontal and vertical waveforms, which is detected by the Doppler signal processor. Kdp is the spatial rate of change of the phase shift, from which can then be inferred information pertaining to water mass and rainrate R(Kdp). An important feature of Kdp is that it depends only on Doppler moments, which can be retrieved accurately even in conditions of partial beam blockage. R(Kdp) is to be applied in the dual-polarization based Echo Classifier (EC) QPE algorithm that is being prepared for WSR-88D operational deployment, for application in areas of large raindrops or hail cores.

A potential problem in utilizing Kdp to estimate precipitation is the considerable amount of statistical noise often found in the Kdp moment. As a spatial derivative of the Doppler phase shift, it is sensitive to noise in either Doppler channel, and thus there is probably a limitation on the degree of beam blockage which it can mitigate. We can also expect signal-to-noise problems to be worse in areas of partial beam blockage, which affect both reflectivity and cross-channel reflectivity correlation – two other moments used in the dual-polarization hydrometeor classifier and QPE algorithms.

Approach

The overall approach is described in detail in the attached Research Project Plan. This work is summarized and concrete examples are presented below.

Since suitable dual polarimetric data are not yet available from the operational WSR-88D, we will use data from the research NCAR S-Pol unit. Apparent partial and total beam blockages are present in two of the recent S-Pol deployments, in Oregon (2001) and Colorado (2006). One deployment was near Boulder, CO for the Refractivity Experiment For H2O Research And Collaborative operational Technology Transfer (REFRACTT2006) and the other in the Oregon Cascades for the Improvement of Microphysical Parameterization through Observational Verification Experiment II (IMPROVEII).

As an introduction to the overall approach, we show relationships among various dual-polarization moments for a previously-evaluated situation in which beam blockage was not a factor.

Figures 1 to 5 depict images from the S-Pol siting near Melbourne, FL, on July 28, 1998 at 2205 UTC. We chose this as our test case because we had done previous work estimating precipitation from an NCAR generated Kdp field during an evaluation of the National Severe Storms Laboratory's dual-pol QPE algorithm in 2006 and 2007. Since then, numerous modifications and improvements have been made to the Kdp computation methodology of that algorithm

Figure 1 shows reflectivity in dBZ for the Melbourne, FL case. There is a large area of precipitation to the north and northeast of the radar, with high-intensity convective echoes along the southern edge and lighter stratiform precipitation to the north. An apparent outflow boundary precedes the convection just to its south. Ground clutter is also noted near the radar site. A sea breeze boundary is depicted running north-south just inland from the coast.

Figure 2 depicts cross correlation coefficient (ρ_{hv}), which is unitless and ranges between 0 and 1, scaled by 1000. It is utilized as a filter, at the 0.9 level, to determine where precipitation is/is not present. Areas of ρ_{hv} greater than 0.9 are shown in red and generally include the entire precipitation area to the north and northeast of the radar. The other echoes noted in Figure 1, such as ground clutter, sea breeze return and outflow

boundary, have ρ_{hv} values less than 0.9 and will therefore not be included in the Kdp estimation.

Figure 3 shows differential phase, Φ, in units of degrees and scaled by 100. Regions other than the area of precipitation to the north and northeast of the radar generally feature a noisy pattern. Some locations in the precipitation area reveal an increase in value of Φ in the radial direction, indicating heavier precipitation along these sections of the radials.

Existing experimental computer code has been modified to compute Kdp and R(Kdp), utilizing the latest methodology (Ryzhkov 2007), that will be implemented in the upcoming WSR-88D Open Radar Product Generator software Build 11.. Results of our Kdp calculation are shown in Figure 4; note that these correspond well to the precipitation region shown in Figures 1-3. The units of Kdp are degrees per kilometer times 100. Only the precipitation area to the north and northeast of the radar has Kdp values computed. Areas of higher reflectivity shown in Figure 1 along the leading (southern) edge of the precipitation have the highest values of Kdp (reds and yellows), as should be the case. There are some negative areas of Kdp, shown in dark blue, in the stratiform region of precipitation, as is possible in areas of decreasing Φ near to (and radially behind) areas of heavy convective precipitation.

Figure 5 shows ρ_{hv} , differential phase Φ, Φ with radial smoothing, and Kdp along one radial, 10 degrees azimuth or toward the NNE. From bin 1 to approximately bin 540 all fields are noisy and ρ_{hv} is less than 0.9, indicating non-precipitation echoes. Therefore, Kdp is not calculated in this range. Between bins 540 and 975 ρ_{hv} is greater than 0.90, indicating precipitation. Kdp is calculated in this range. In association with the convection along the leading edge of the precipitation, Φ increases abruptly and then quickly decreases at nearly the same rate (approximately between bins 540 and 700). Therefore Kdp, the rate of change of Φ, becomes large-positive with the increase of Φ, and then becomes negative as Φ decreases. In this area, since reflectivity (not shown) is greater than 40 dBZ, short gate smoothing and linear least squares fit are used in computing Kdp, in accordance with the algorithm enunciation language (AEL) for the operational, dual-polar precip algorithm. For the remainder of the precipitation area from about bin 700 to 1000, Φ generally increases slowly, with occasional small fluctuations. Thus, Kdp is generally small and positive in this stratiform precipitation region. In this range, since reflectivity is generally less than 40 dBZ, long-gate smoothing and linear least squares fit are used, following the current AEL. Beyond about bin 1000, ρ_{hv} falls below 0.9 as this range is north of the precipitation area and therefore, Kdp is not computed.

A similar set of illustrations is then presented for one of the S-Pol deployments utilized in the present study, featuring partial or total blockage over large sectors of the umbrella. Figures 6-10 show images from the S-Pol when it was sited in the Oregon Cascades on November 28, 2001 at 0640 UTC, at an elevation of 0.5 degrees. At this time, precipitation was extensive throughout this area and – in the absence of blockage – widespread echoes would be expected to be visible across the radar umbrella.

In Figure 6 (Reflectivity), large regions of total beam blockages and apparent partial beam blockages are evident (i.e. black or blank), with total beam blockage most notable in a swath about 45 degrees wide to the north-northwest of the radar and another about 20 degrees wide to its south-southwest. Intermittent swaths of total beam blockage are also apparent throughout the eastern sector of the radar umbrella, intermingled with swaths of partial beam blockage. Promising areas of partial beam blockage are also evident to the south and southwest, to either side of the area of total or near total blockage mentioned above. Another area of partial blockage appears in a narrow sector to the west-northwest of the radar. Locations with one-hour and 15-minute time interval rain gauge data are plotted in Figure 6, as well. Note that there are apparently numerous gauges in unblocked and partially blocked regions.

Figures 7 (cross correlation coefficient, ρ_{hv}) and 8 (differential phase, Φ) assist in the identification of the blockage characteristics, described above, at 0.5 degrees elevation, with the sectors inferred to have the most blockage appearing the most blue (i.e. lowest ρ_{hv}) in Figure 7 and the most speckled (i.e. least horizontally consistent Φ) in figure 8.

Results of our Kdp calculation are shown in Figure 9 and correspond well to the (non-blocked) precipitation regions shown in Figures 6-8. However, note that with the current, rather stringent threshold settings for algorithm parameters such as radial smoothing, ρ_{hv}, and Z minimum, only the radials with no or very little blockage meet the criteria that allow for Kdp computation. We will most likely have to tweak these thresholds to enable more significant areas of Kdp to be computed in the partially blocked regions. Investigations continue in this area.

Figure 10 shows ρ_{hv}, Φ, smoothed Φ, and Kdp along one radial that experienced rainfall through much of its length, i.e. 285 degrees azimuth, or toward the WNW. In this case, from approximately bins 320 to 700, the Φ moment increases nearly monotonically with distance, and the Kdp trace remains positive throughout this range.

Figures 11-15 are for the same case as in Figures 6-10 except at the next higher elevation, 1.5 degrees. Note that partial and total beam blockage are much less pronounced at this elevation, while high values of reflectivity are still present, indicative of widespread and significant precipitation. The presence of non-blocked precipitation above partially blocked should allow deductions to be made regarding precipitation estimates determined from the various sources (e.g. R(Kdp); R(Zh); R(Zh, Zdr)) in the sectors below (i.e. at 0.5 deg).

(Note: the appearance of a spiral zone of low Kdp south and west of the radar in Figure 14 is being investigated; it might be a data processing artifact.)

Future Work

Similar illustrations as Figs 6-15 will be assembled from the S-Pol deployment in Colorado for a rain event in the summer of 2006. The R(Kdp) fields from both locations

will be evaluated in the following ways. First, one-hour rainfall fields will be constructed for the mixed blocked-unblocked antenna elevation angles (e.g. 0.5 and 1.5 degrees) using Zh, Zh-Zdr, and Kdp rainfall algorithms (Ryzhkov et al 2005c). These fields will be visually assessed for changes in horizontal continuity across annular sectors (i.e. in the azimuthal direction, at fixed range) as conditions vary from blocked to partially blocked to unblocked (with the expectation that R(Kdp) will show more coherence between unblocked and partially blocked regions than R(Zh) or R(Zh,Zdr)).

Next we will compare the various measures of QPE from S-Pol to "ground truth" fields based on rain gauges. To accomplish this, we will obtain all available rain gauge reports from the umbrella as a whole and perform gauge/radar comparisons on a point-by-point basis, or we will acquire and evaluate Stage III, Stage IV, or other continuous gridded precipitation fields for the same events, depending on availability. For the Colorado radar deployment, Stage IV multisensor data is available; for the Oregon deployment, we have a daily raingauge analysis prepared by the NCEP Climate Prediction Center, which could be disaggregated to 1-h or 6-h amounts by tracking based on data from the KRTX (Portland OR) and KMAX (Medford OR) WSR-88D units. If only the 6-hour data are available, we will disaggregate it to 1-hour elements by analogy to the fractional, hourly amounts in nearby areas with unblocked S-Pol coverage, or from the corresponding rainfall estimates from Zh itself in the same areas. Another alternative would be to collect S-Pol accumulations for 6-hour periods and base conclusions on comparisons with the Stage IV, itself.

From these alternative precipitation data sources we will make the following comparisons:

1. Is the relationship between R(Kdp) and the "ground truth" field fairly constant between the blocked and unblocked areas? This would indicate R(Kdp) is useful to improve QPE in partial beam blockage conditions.
2. Is the relationship between R(Kdp) and R(Zh) or R(Zh, Zdr) at the next higher elevation more or less the same in the blocked vs. unblocked areas? Again, R(Kdp) should be more consistent between the blocked and unblocked regions. This would indicate Kdp itself is not as sensitive to partial beam blockage.
3. Can we even estimate lighter rainfall effectively from R(Kdp) alone? In dual-polar QPE algorithms (such as that soon to be implemented operationally for the WSR-88D), R(Kdp) is utilized only in areas where large raindrops or hail are assumed present. The limited literature indicates that for rain rates less than 8 mm/hour, R(Kdp) is likely too noisy to effectively estimate rainfall, and R(Zh) is better. Since the WSR-88D dual-polar QPE and hydrometeor classifier algorithms were developed from the KOUN, experimental radar in an essentially flat-terrain, blockage-free region of Oklahoma, we must determine if various assumptions, such as the use of ρ_{hv} as a precipitation indicator, are still valid in partially blocked sectors.

References

Friedrich, K., Germann, U., Gourley, J., Tabary, P., 2007: Effects of Radar Beam Shielding on Rainfall Estimation for the Polarimetric C-band Radar. *J Atmos. and Ocean. Tech*., **24**, 1839-1859.

Ryzhkov, A., 2007: Dual Polarimetric Preprocessor Algorithm Description NX-DR-03-061.

Ryzhkov, A., Giangrande, S., Melnikov, V., and Schuur, T., 2005a: Calibration Issues of Dual-Polarization Radar Measurements. *J Atmos. and Ocean Tech*., **22**, 1156-1166.

Ryzhkov, A., Giangrande, S., and Schuur, T., 2005b: Rainfall estimation with a polarimetric prototype of WSR-88D. *J of Appl. Meteor.*, **44**, 502-515.

Ryzhkov, A., Schuur, T., Burgess, D., Heinselman, P., Giangrande, S, and Zrnic, D., 2005c: The Joint Polarization Experiment: Polarimetric Rainfall Measurements and Hydrometeor Classification. *Bull. Amer. Meteor. Soc*. **86**, 809-824.

Ryzhkov, A., Zrnic, D., 1998: Polarimetric Rainfall in the Presence of Anomalous Propagation., *J Atmos. and Ocean Tech.* **15**, 1320-1330.

Vivekanandan, J., Yates, D., and Brandes, E., 1999: The influence of terrain on rainfall estimates from radar reflectivity and specific propagation phase observations. *J Atmos. and Ocean. Tech*., **16**, 837-845.

Zrnic, D., Ryzhkov, A., 1996: Advantages of Rain Measurements Using Specific Differential Phase. *J of Atmos and Ocean Tech*., **13**, 454-463.

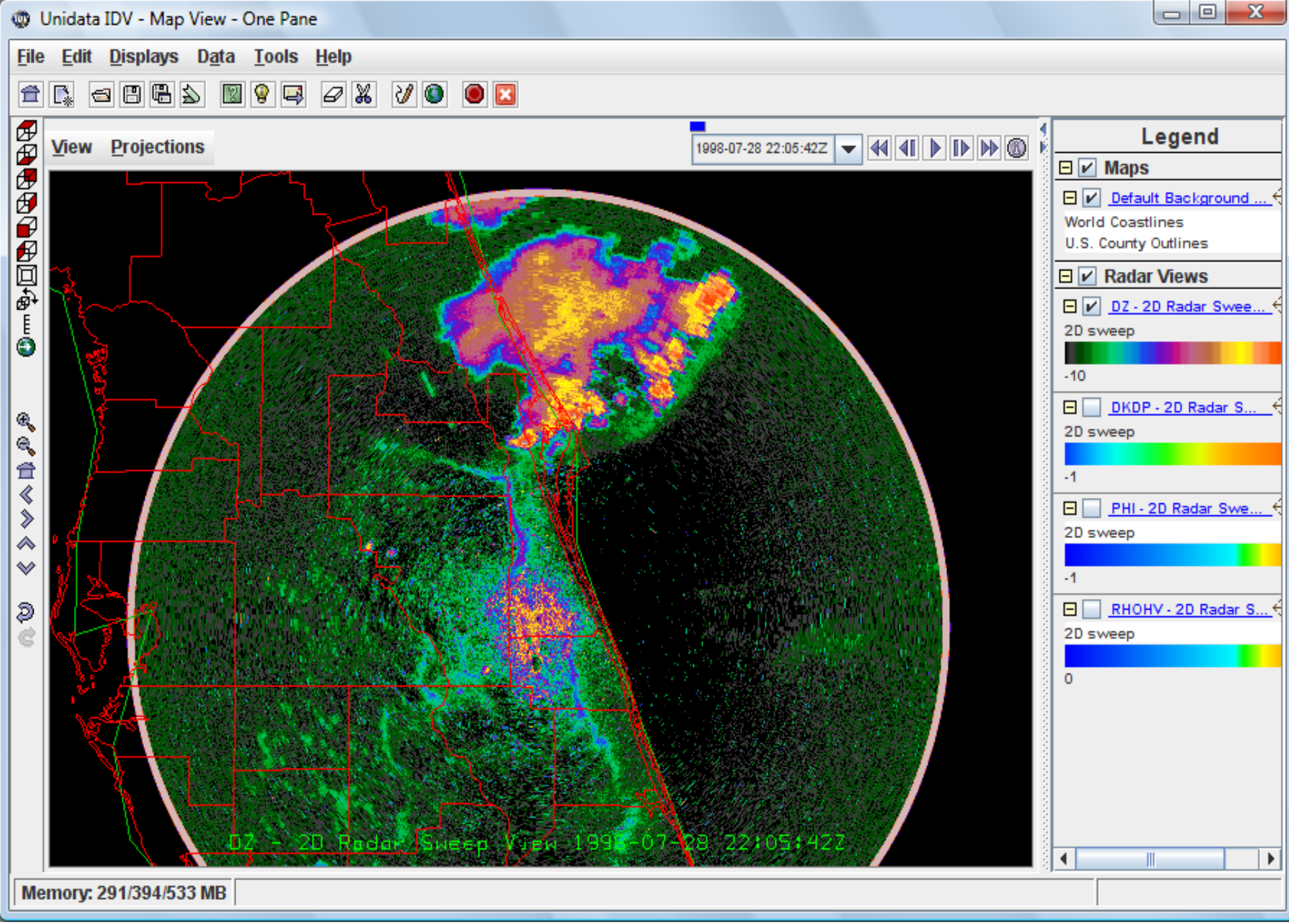

Figure 1. Reflectivity from S-Pol location near Melbourne, FL July 28, 1998 2205 UTC

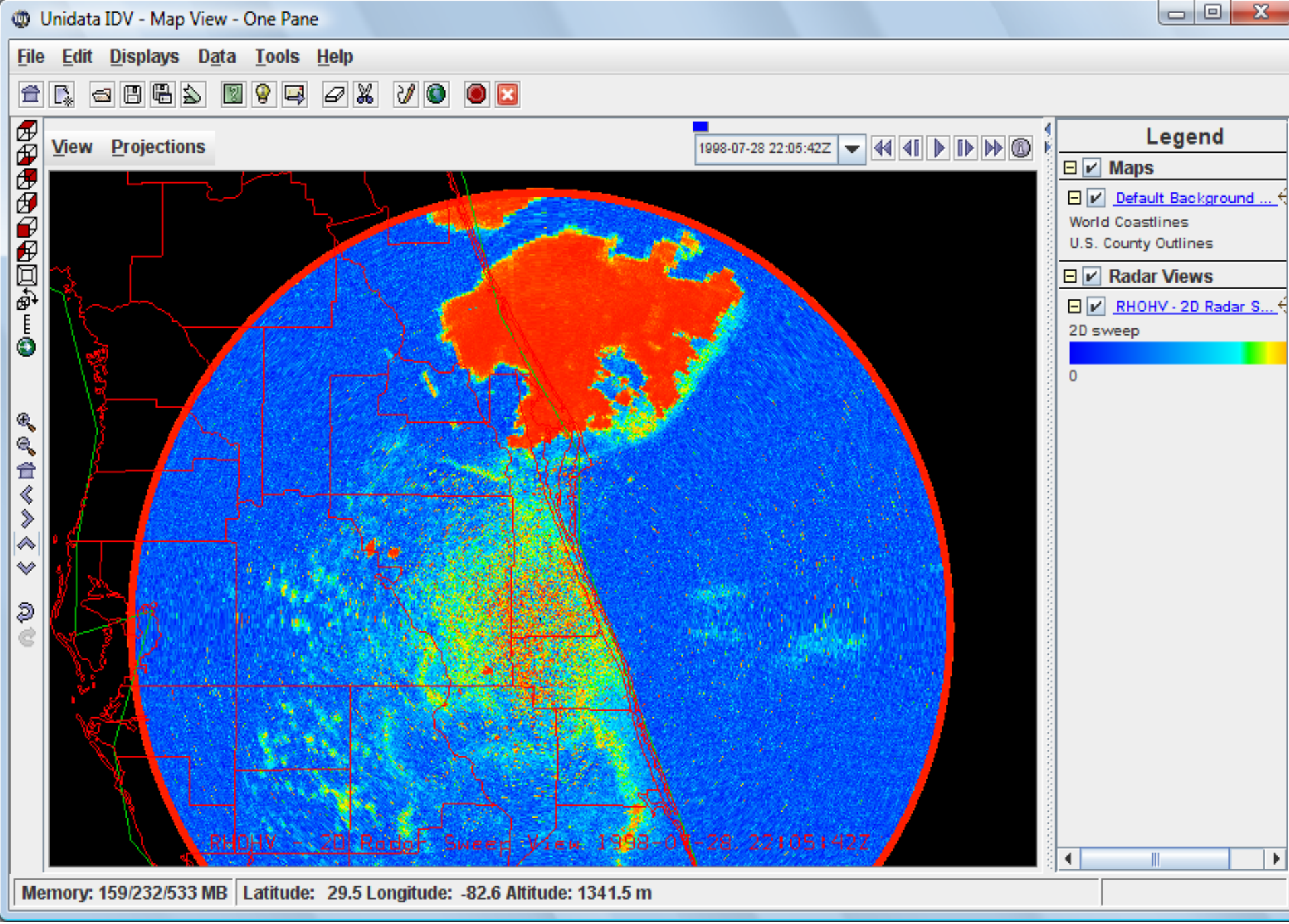

Figure 2. Same as figure 1 except for Correlation Coefficient (ρhv)

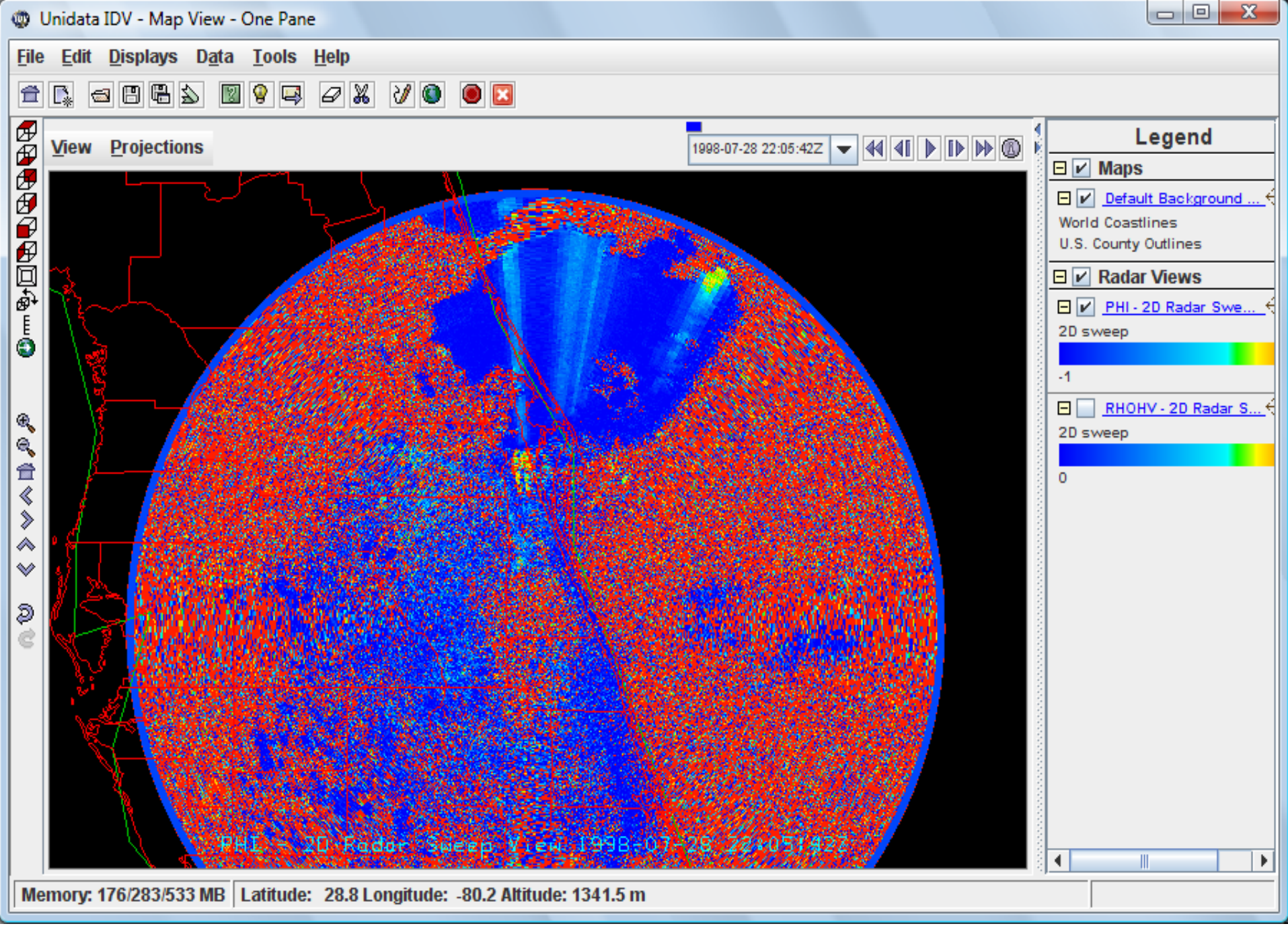

Figure 3. Same as figure 1 except for Differential Phase (Φ)

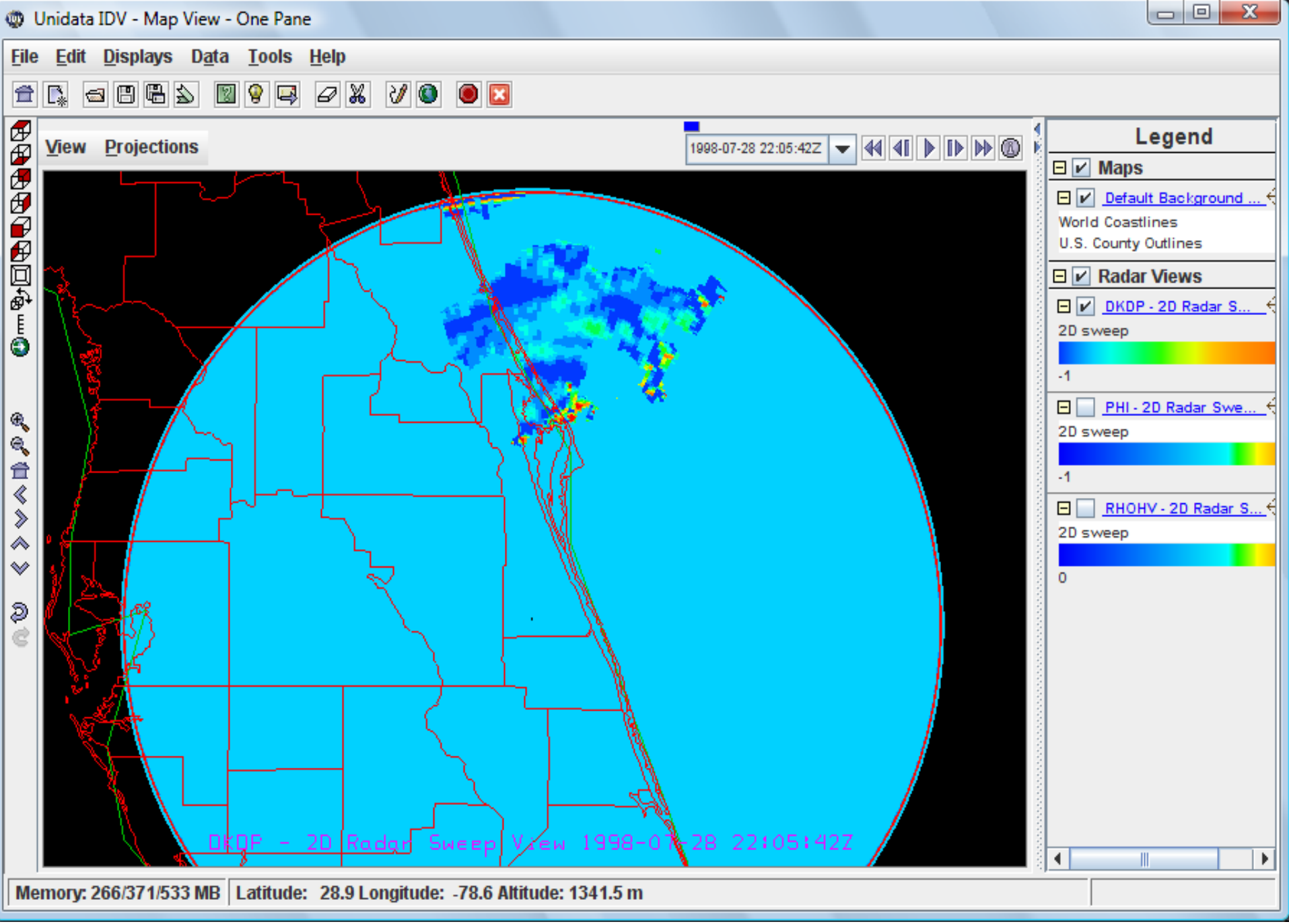

Figure 4. Same as Figure 1 except for calculated Specific Differential Phase (K_{DP})

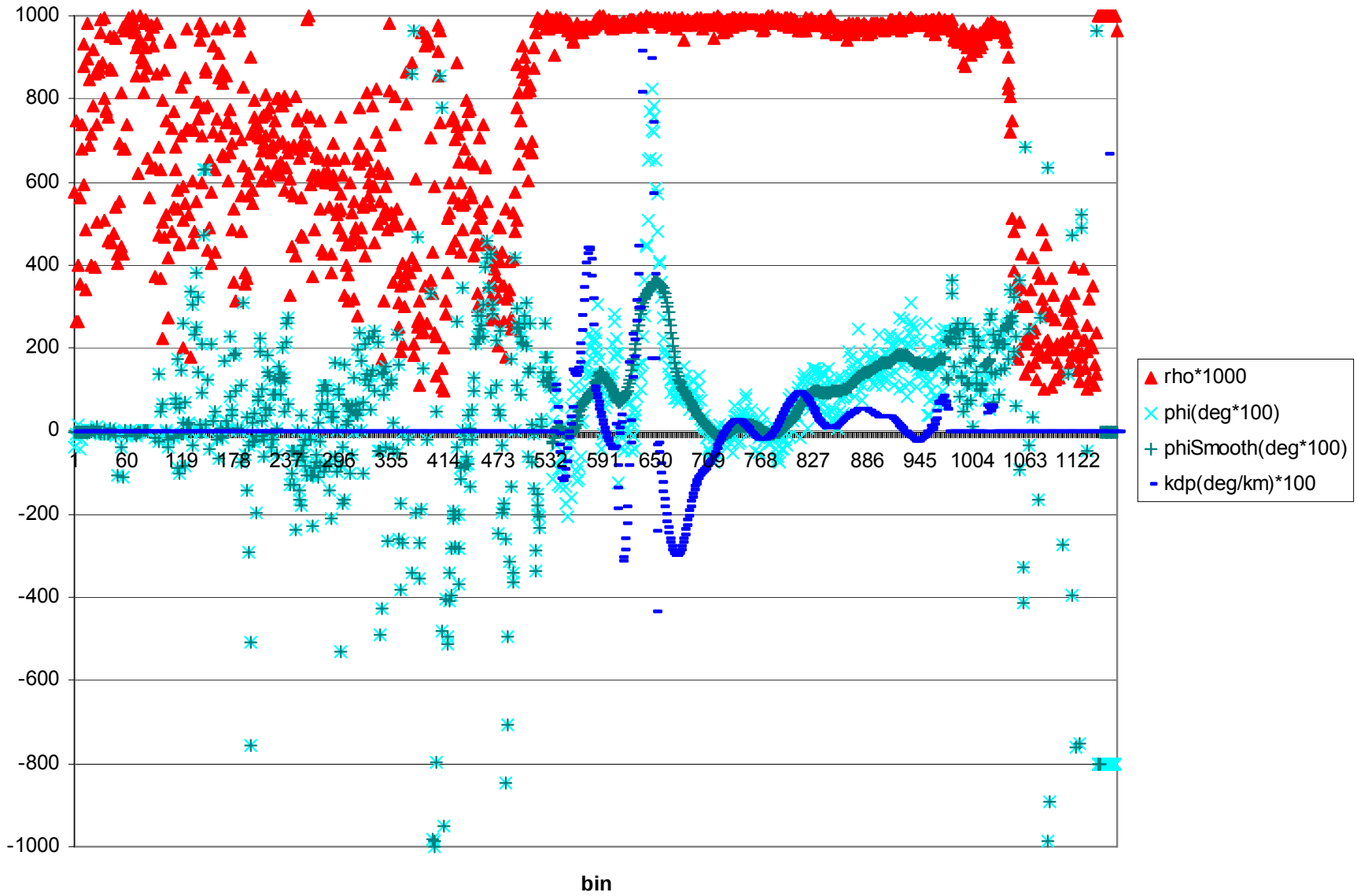

Figure 5. Values of RHO, PHI, smoothed PHI and calculated KDP along radial 010 degrees Azimuth for case shown in Figs 1-4. Precipitation region extends from approximately bin 540 to bin 975. Since Z(not shown) was greater than 40 dBz in bins ~540 to 650 short gate smoothing was used. Elsewhere long gate smoothing was used.

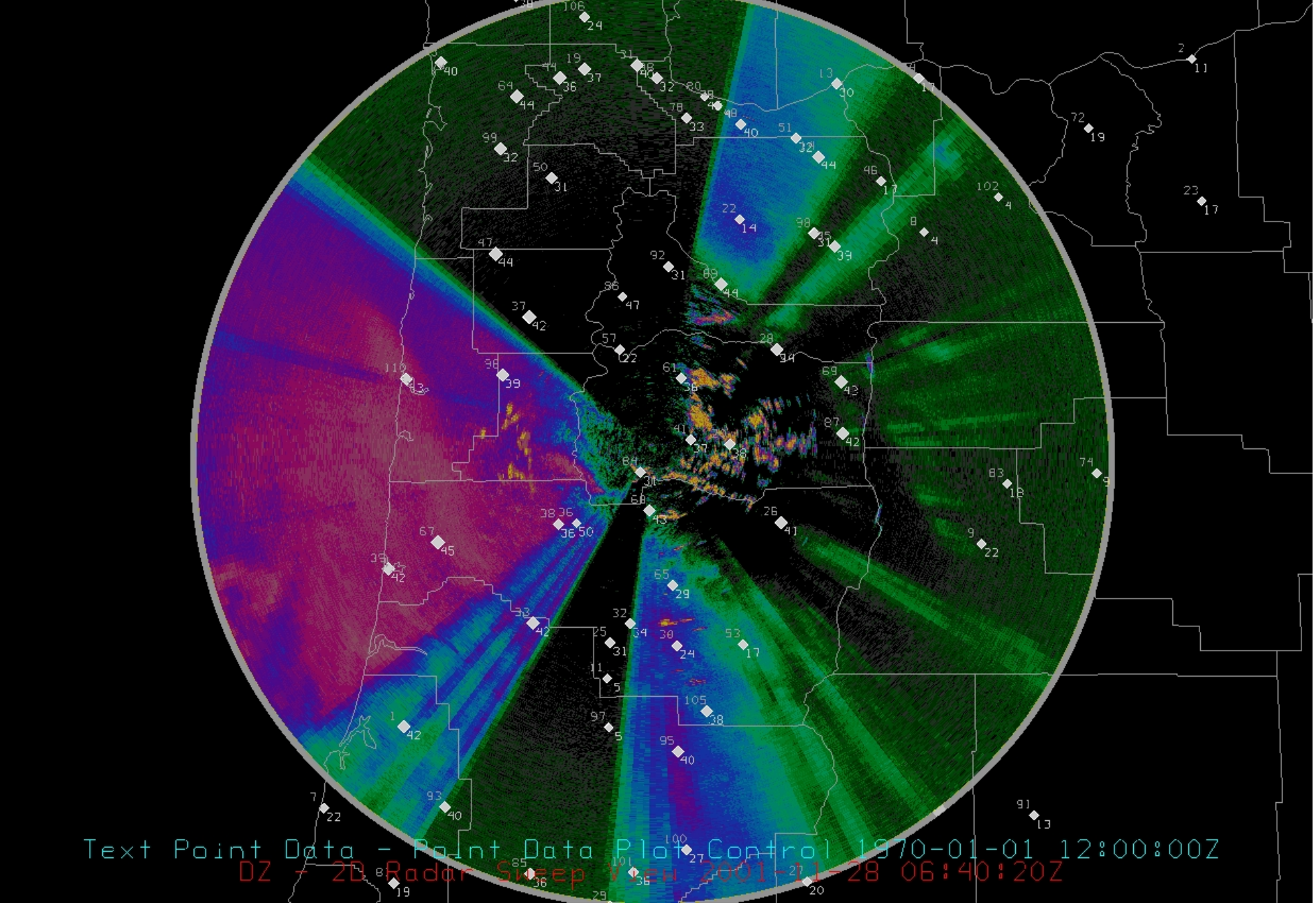

Figure 6. Reflectivity from S-Pol location in the Oregon Cascades on November 28, 2001 at 0640 UTC at 0.5 degree elevation. White diamonds indicate gauge locations. Gray numbers on the top left indicate number of 15-minute periods available for the event while the white number at the lower right of the diamond indicates number of hourly periods.

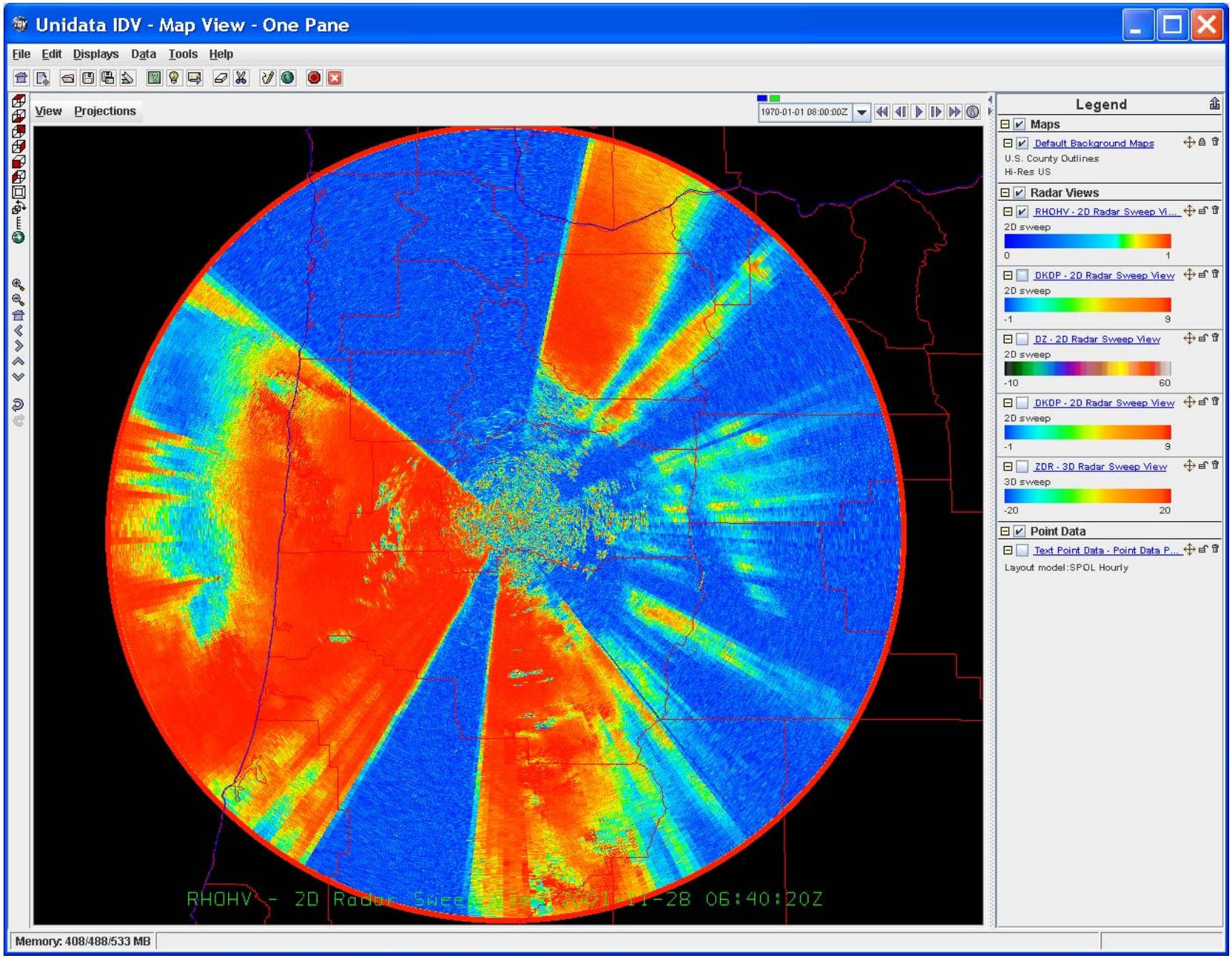

Figure 7. As in Figure 6 except for ρ_{hv}.

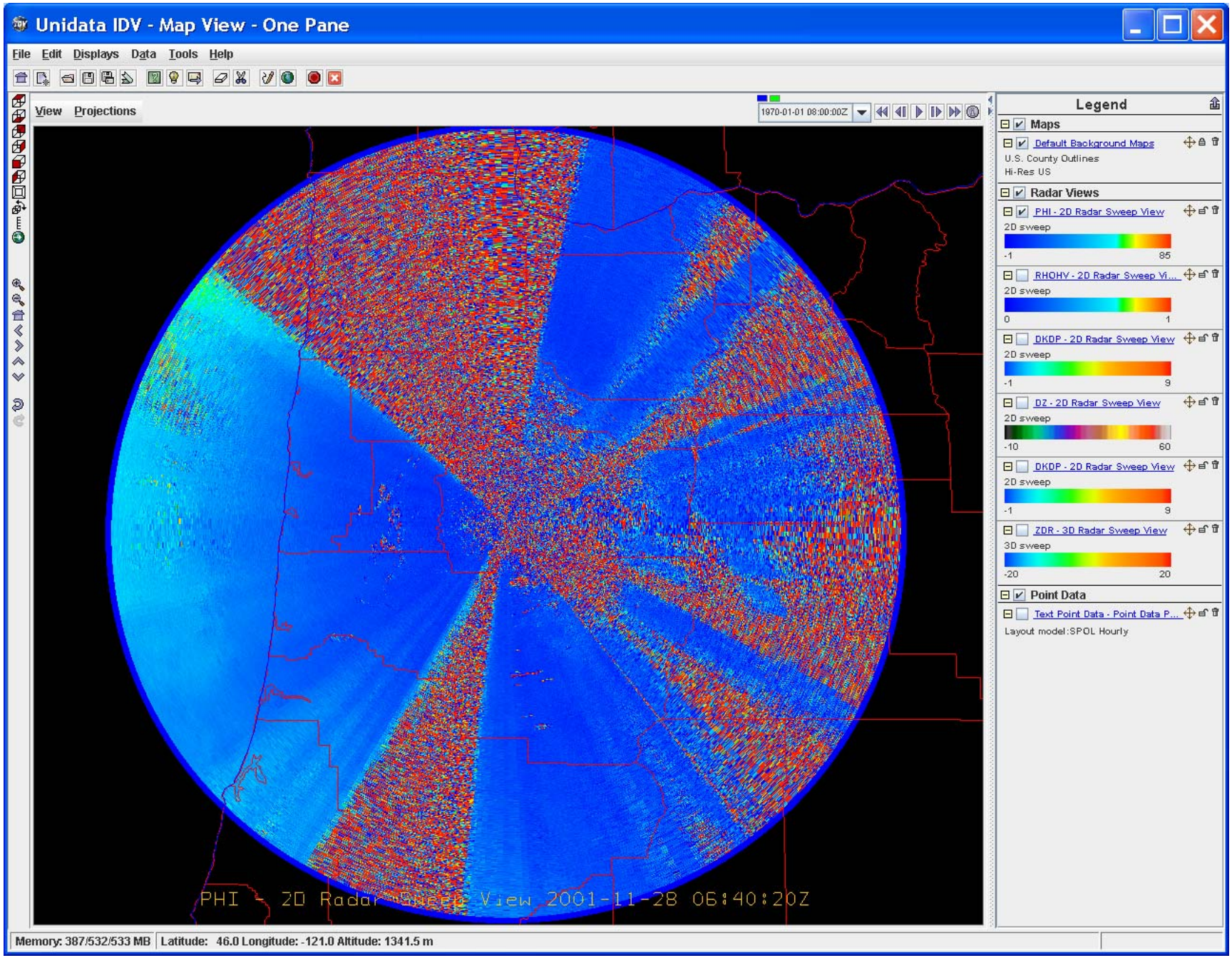

Figure 8. As in Figure 6 except for Φdp.

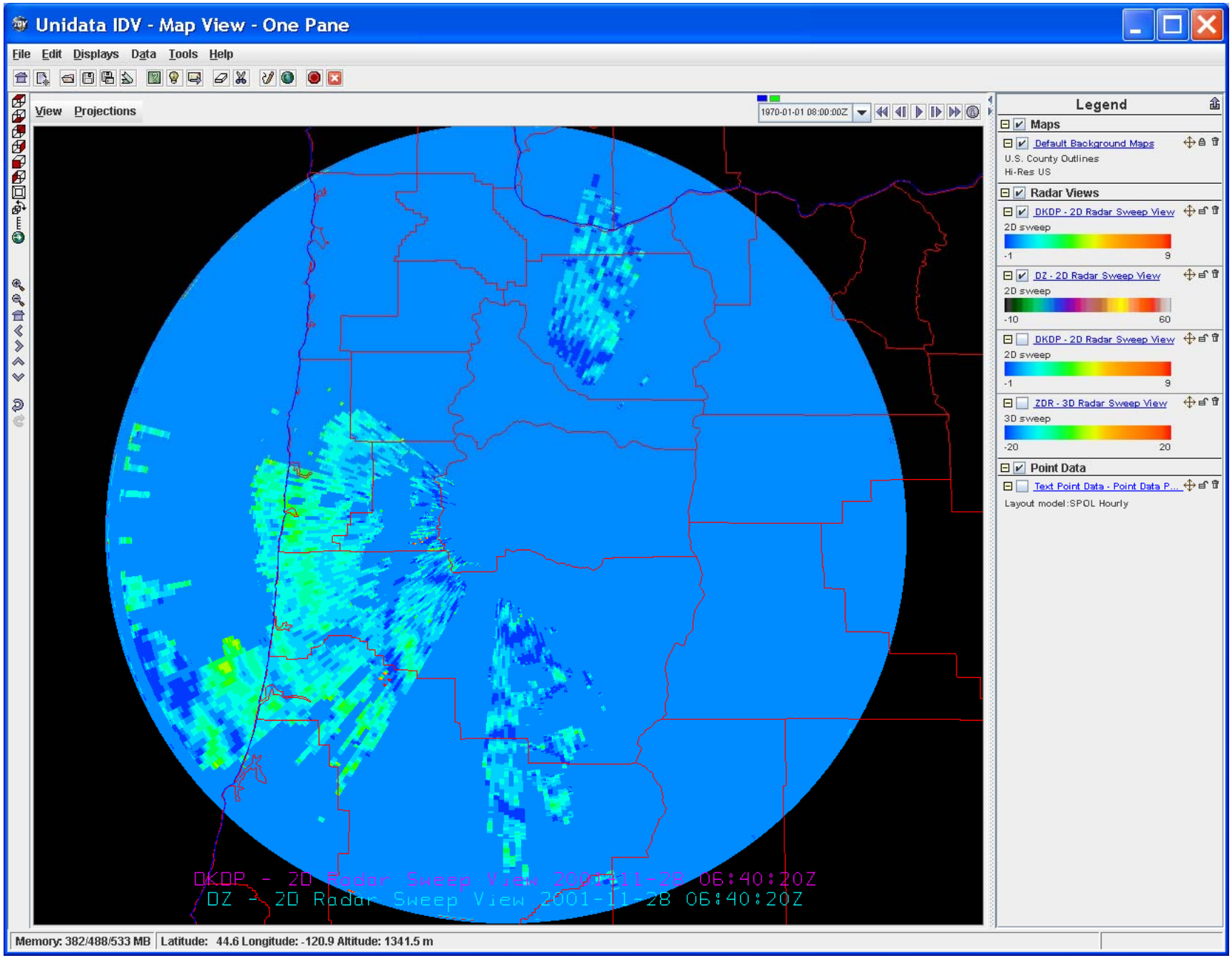

Figure 9. As in Figure 6 except for Kdp.

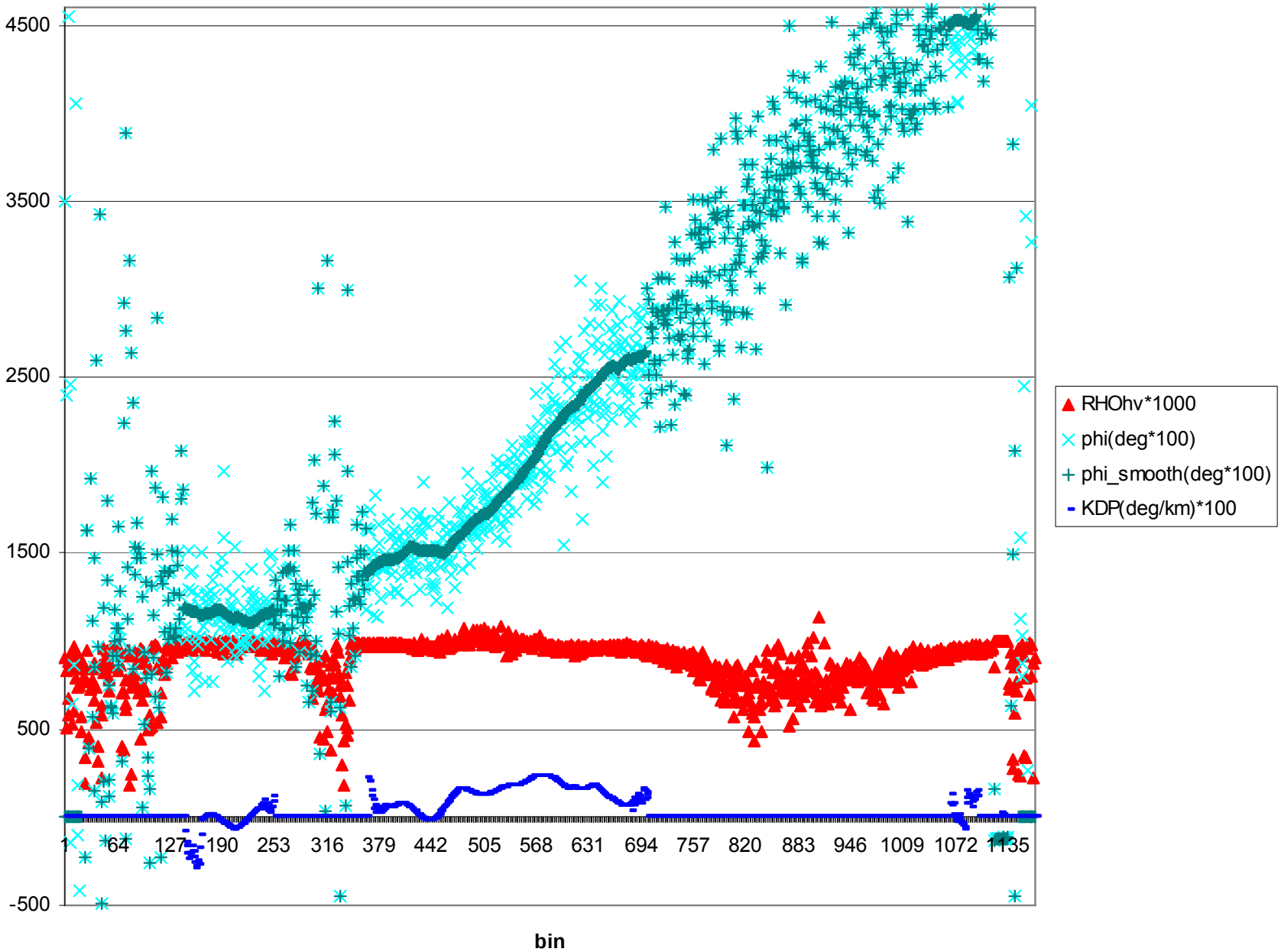

Figure 10. Values of RHO, PHI, smoothed PHI and calculated KDP along radial 285 degrees Azimuth for case shown in Figs 6-9.

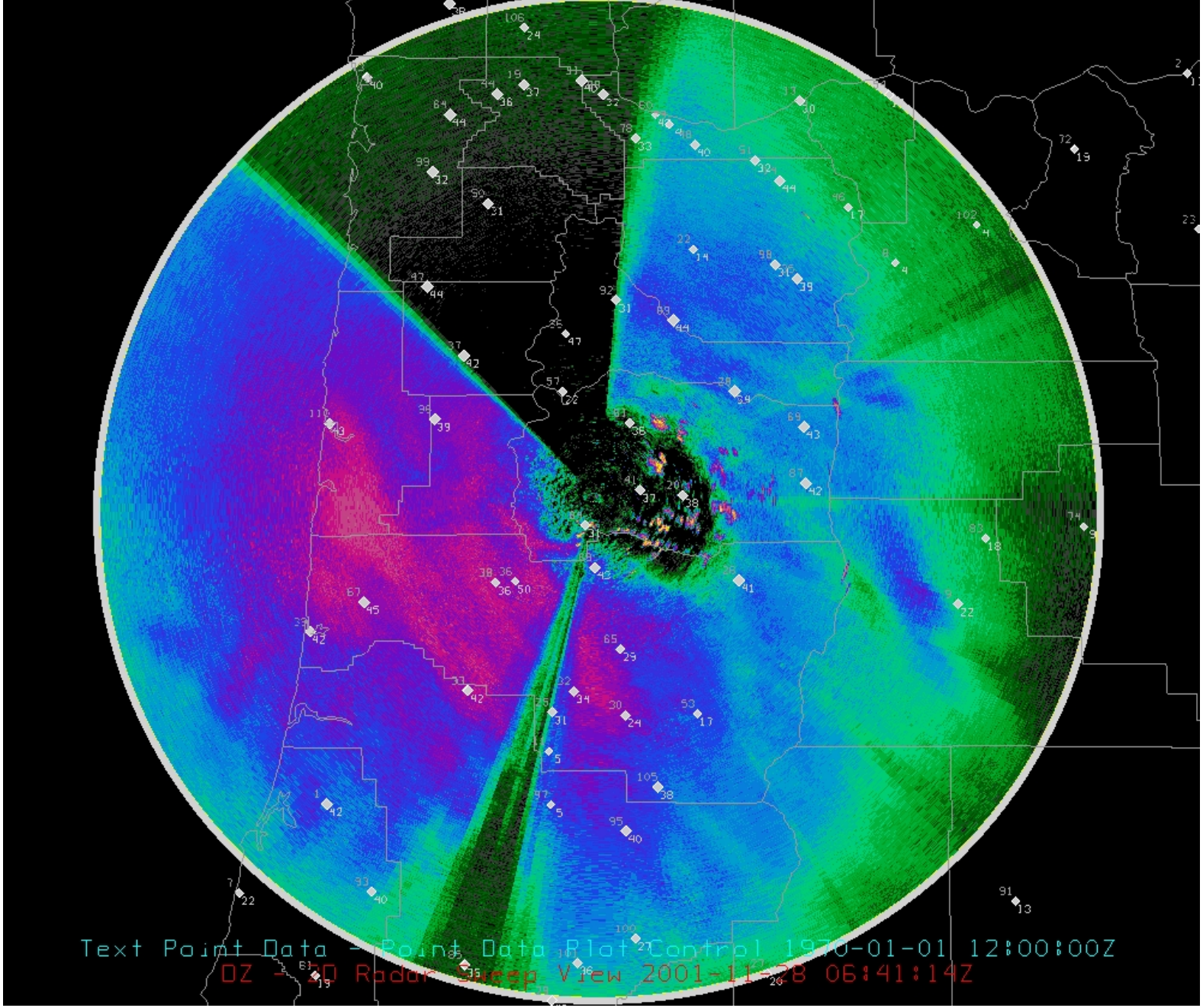

Figure 11. Reflectivity field, same as figure 6 except 1.5 degree elevation.

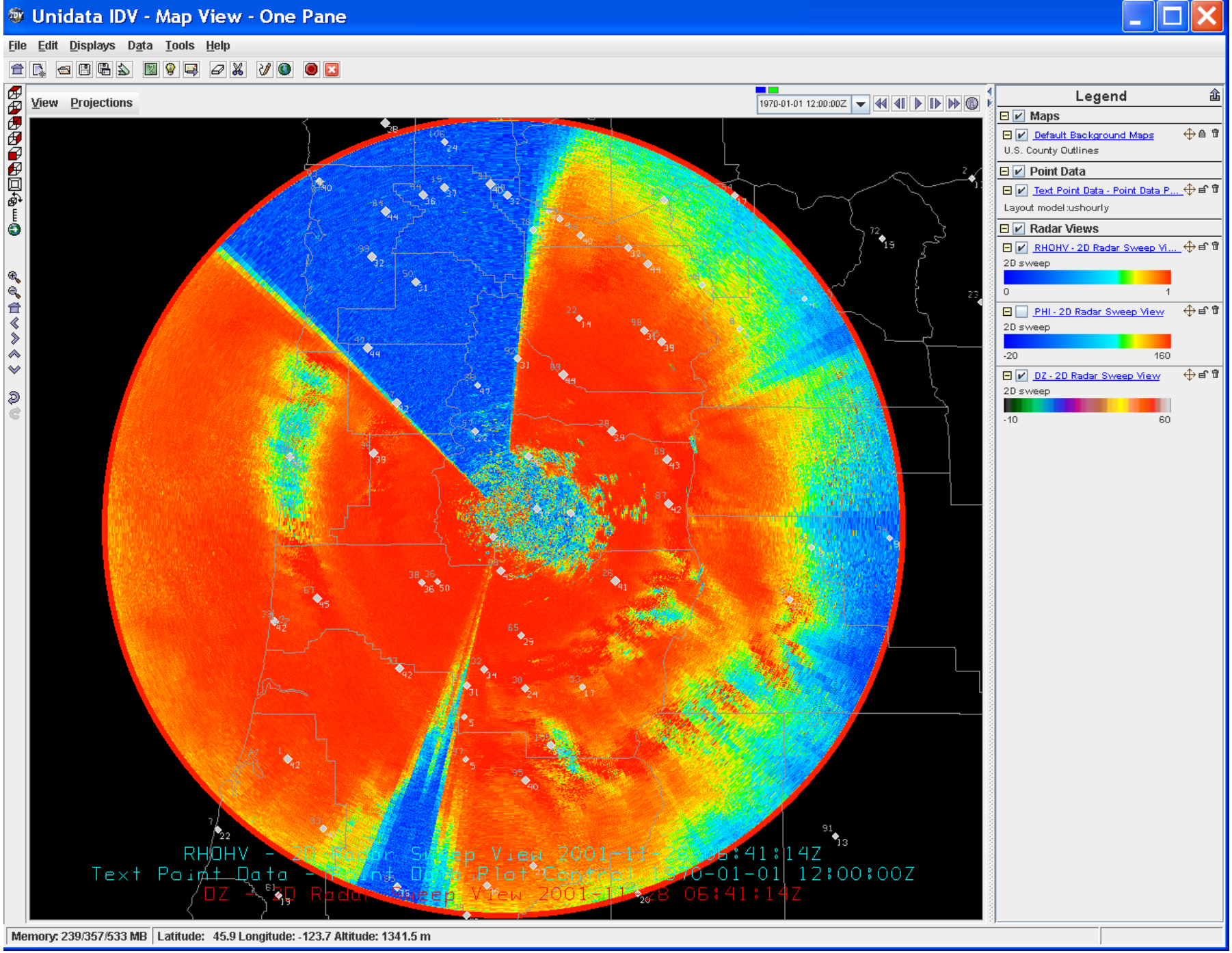

Figure 12. ρ_{hv} field, same as figure 7 except 1.5 degree elevation.

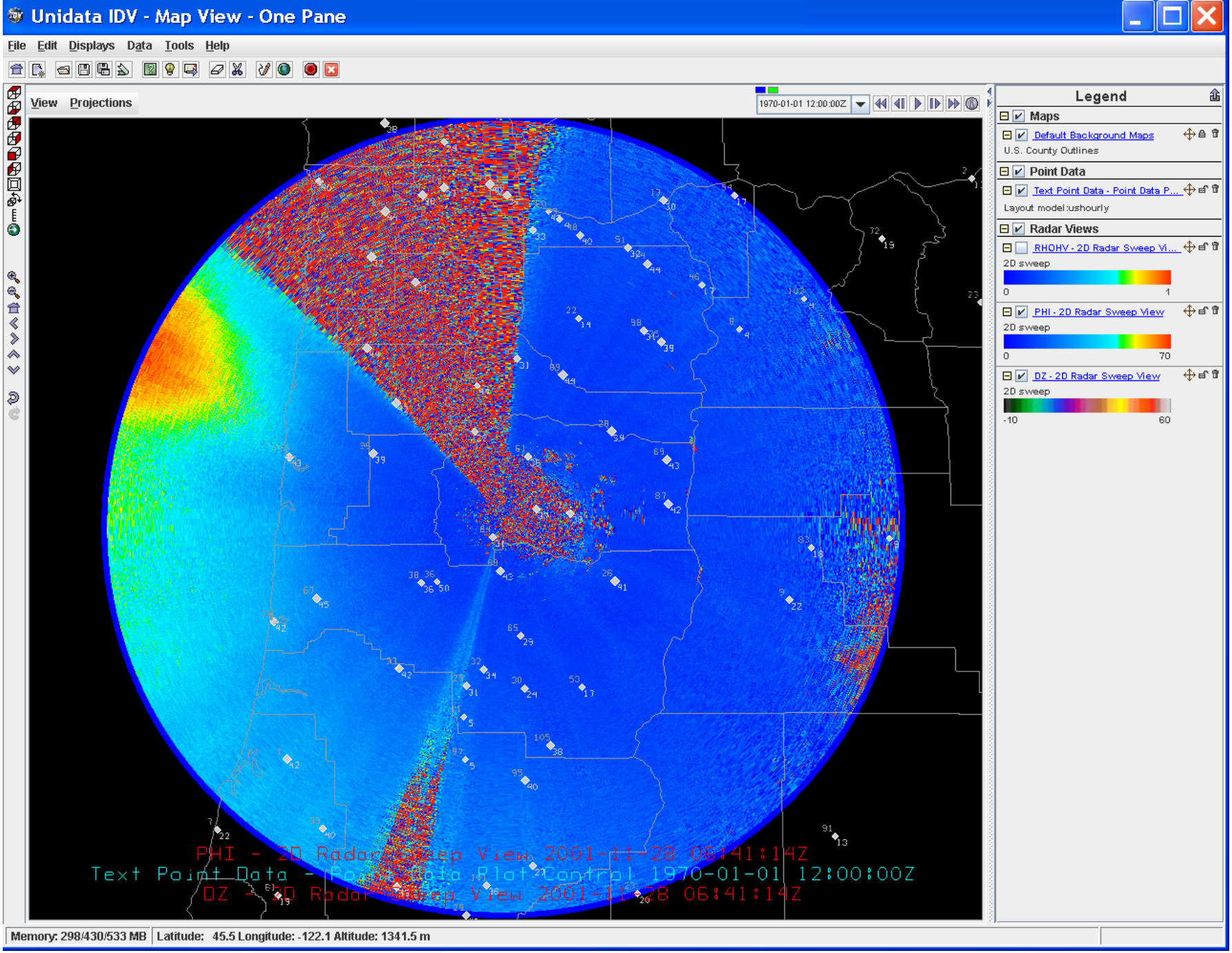

Figure 13. Φdp field, same as figure 8 except 1.5 degree elevation.

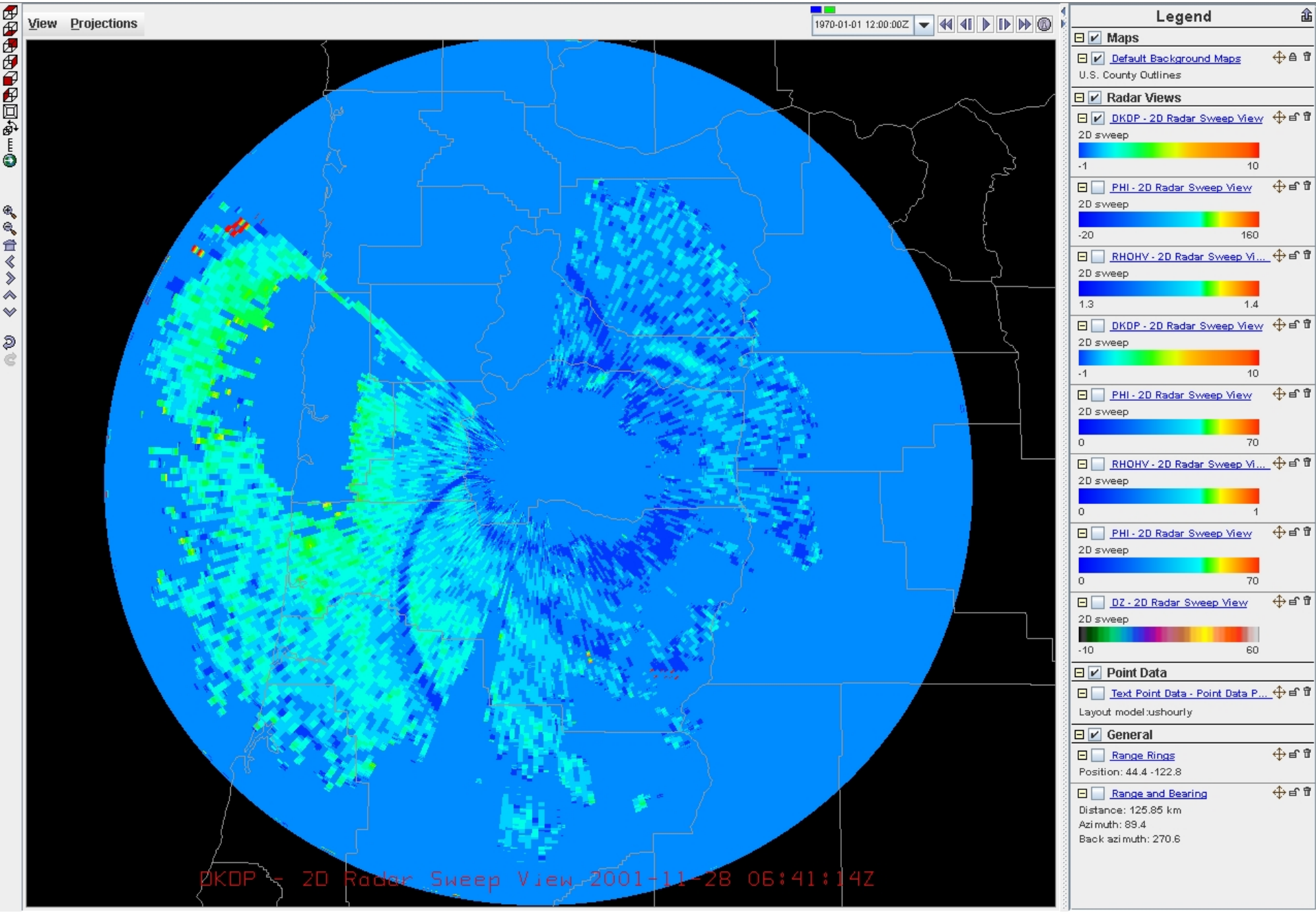

Figure 14. Kdp field, same as figure 9 except 1.5 degree elevation.

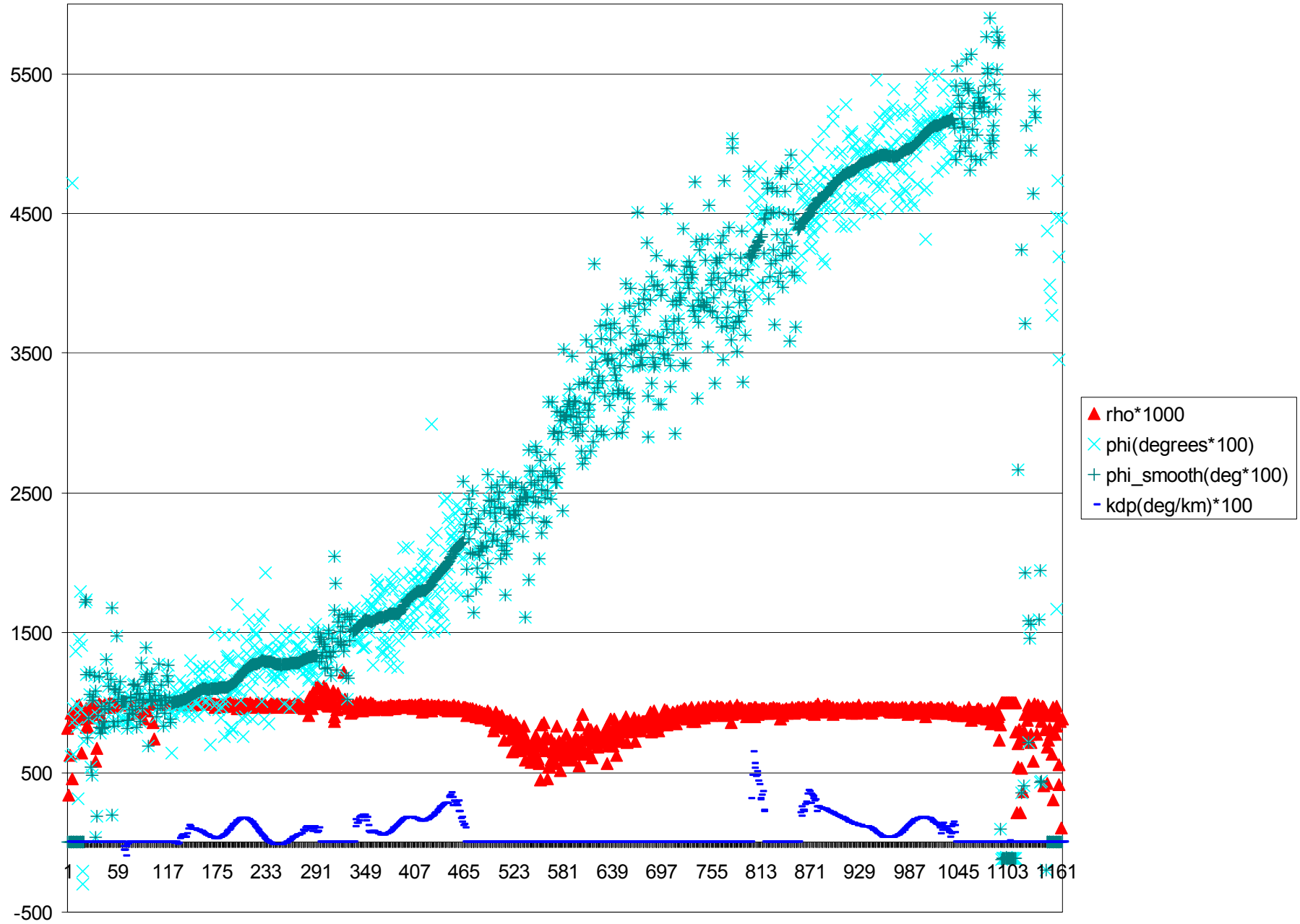

Figure 15. Same as figure 10 except for 1.5 degree elevation.